

# Rapid Generation of Biologically Relevant Hydrogels Containing Long-Range Chemical Gradients

By Jiankang He, Yanan Du, José L. Villa-Uribe, Changmo Hwang, Dichen Li, and Ali Khademhosseini\*

Many biological processes are regulated by gradients of bioactive chemicals. Thus, the generation of materials with embedded chemical gradients may be beneficial for understanding biological phenomena and generating tissue-mimetic constructs. Here a simple and versatile method to rapidly generate materials containing centimeter-long gradients of chemical properties in a microfluidic channel is described. The formation of a chemical gradient is initiated by a passive-pump-induced forward flow and further developed during an evaporation-induced backward flow. The gradient is spatially controlled by the backward flow time and the hydrogel material containing the gradient is synthesized via photopolymerization. Gradients of a cell-adhesion ligand, Arg-Gly-Asp-Ser (RGDS), are incorporated in poly(ethylene glycol)-diacrylate (PEG-DA) hydrogels to test the response of endothelial cells. The cells attach and spread along the hydrogel material in a manner consistent with the RGDS-gradient profile. A hydrogel containing a PEG-DA concentration gradient and constant RGDS concentration is also shown. The morphology of cells cultured on such hydrogel changes from round in the lower PEG-DA concentration regions to well-spread in the higher PEG-DA concentration regions. This approach is expected to be a valuable tool to investigate the cell–material interactions in a simple and high-throughput manner and to design graded biomimetic materials for tissue engineering applications.

adhesion, locomotion and gene expression.<sup>[1–6]</sup> Thus, the ability to recreate and study such interactions may facilitate the development of bioactive and biomimetic materials for various biological and biomedical applications.<sup>[1,7]</sup> Numerous studies have shown that both chemical and physical properties of the matrix materials are important to determine the cellular behavior in the surrounding natural or artificial microenvironments.<sup>[8]</sup> It should be noted that most previous investigations of the cell–material interactions have used individual material samples with uniform chemical or physical properties, which limits the number of samples for testing and their application in studies that require continuous variations in the material properties (chemical or physical), such as haptotaxis<sup>[9,10]</sup> or durotaxis.<sup>[11,12]</sup> Most of the biomaterials designed for tissue-engineering applications also lack the spatially and structurally defined anisotropic properties that exist in native tissues.<sup>[13,14]</sup> Biomaterials with a continuous variance in properties are, therefore, of great interest to create biomimetic cellular niches for biological investigations and tissue-engineering

## 1. Introduction

Interactions between cells and materials have been shown to profoundly regulate the characteristics, such as morphology,

applications.<sup>[15,16]</sup>

Numerous approaches have been adopted to engineer material gradients with chemical variance, including manipulating the diffusion pattern or duration of exposure of the photocrosslinkable materials to UV or laser irradiation,<sup>[17–19]</sup> electrochemistry,<sup>[20,21]</sup> plasma polymerization,<sup>[22,23]</sup> fluidic gradient mixers,<sup>[24,25]</sup> and microfluidic gradient generators.<sup>[2,5,26,27]</sup> However, most of the approaches mentioned above require long and sophisticated fabrication procedures involving expertise and expensive equipment. In addition, it is normally difficult to generate long-range material gradients, which will increase the number of conditions and accuracy for the quantitative investigation of cell–material interactions, and graded materials for tissue engineering applications.<sup>[28]</sup> For example, to generate long-range hydrogel gradients by pure diffusion, it may take several days to establish a gradient of the desired molecules from the source to the sink before polymerization. In the case of microfluidic gradient generators, the length of the gradient is determined by the combined length of all the input streams. Thus, in order to generate a centimeter-long gradient, a complicated microfluidic network containing a large number

[\*] Prof. A. Khademhosseini, J. He, Dr. Y. Du, J. L. Villa-Uribe, Dr. C. Hwang

Center for Biomedical Engineering  
Department of Medicine  
Brigham and Women's Hospital  
Harvard Medical School  
Boston, MA, 02115 (USA)  
E-mail: alik@rics.bwh.harvard.edu

Prof. A. Khademhosseini, J. He, Dr. Y. Du, J. L. Villa-Uribe, Dr. C. Hwang  
Harvard-MIT Division of Health Sciences and Technology  
Massachusetts Institute of Technology  
Cambridge, MA, 02139 (USA)

Prof. D. Li, J. He  
State Key Laboratory of Manufacturing Systems Engineering  
Xi'an Jiaotong University  
Xi'an, Shaanxi, 710049 (P. R. China)

DOI: 10.1002/adfm.200901311

of input streams will be required. Such technical difficulties may be the reason that previous microfluidic-based techniques have been limited to generating gradients that were only a few hundred micrometers in size.

We have developed a rapid and simple microfluidic-based approach to generate gradient of chemical properties within biologically relevant hydrogels. By integrating portable microfluidic manipulation and photopolymerization, a hydrogel gradient can be rapidly achieved with minimal requirements in cost or expertise. The size of such gradients is on the centimeter length scale, which has been difficult to achieve by most of the existing methods. Our approach for making materials with embedded chemical gradient is based on using a portable microfluidic device for generating a molecular concentration gradient, which is initiated by a passive-pump-induced forward flow and further developed during an evaporation-induced backward flow.<sup>[29]</sup> Here we engineered spatially controlled centimeter-long hydrogels by initially generating a concentration gradient of photo-crosslinkable hydrogel precursors, which contain a mixture of PEG-DA, photoinitiator, and/or PEG derivative of the cell-adhesive peptide RGDS (acryloyl (Acr)-PEG-RGDS) in the microfluidic device. The concentration gradient (either Acr-PEG-RGDS gradient or PEG-DA gradient) was photopolymerized later to form the material gradient with variance in either RGDS concentration or PEG-DA concentration. This microfluidic-based material gradient approach enables the rapid and easy generation of biomaterials with a continuous variance in concentration, cell adhesiveness, and porosity, which is envisioned to be a powerful tool for a wide range of biological and tissue-engineering applications.

## 2. Results

The gradient-generation and stabilization processes are illustrated in Figure 1. The gradient materials were generated inside a fluidic channel that was formed by reversibly sealing a polydimethylsiloxane (PDMS) mold, containing the impression of the channel, onto a glass slide (Fig. 1A). The channel was first pre-filled with PEG-DA solution from the outlet. Then, 6  $\mu\text{L}$  of PEG-DA solution containing the chemicals of interest were introduced from the inlet (Fig. 1B). The forward flow rate was measured to be  $1 \text{ mm s}^{-1}$ , which did not cause leaking from the reversibly sealed fluidic channel (Fig. 1C). The gradient was generated during the period of evaporation-induced backward flow (Fig. 1D). The backward flow was stopped by placing the fluidic system into a humidified chamber, and subsequently the hydrogel precursors were photopolymerized to form the gradient hydrogel (Fig. 1E). As shown in Figure 1F, the resultant hydrogel is comprised of three different regions: 1) a positive control region with bioactive chemicals of interest or the highest PEG-DA concentration, 2) a centimeter-long gradient region, and 3) a negative control region with no bioactive chemicals of interest or the lowest PEG-DA concentration.

Several factors were essential to create the centimeter-long gradient hydrogel. First, the PDMS mold should be hydrophobic to maintain the spherical shape of the droplets, which is critical to enable the passive-pumping process. Therefore, the PDMS mold should not be plasma treated. Second, the length of the gradient

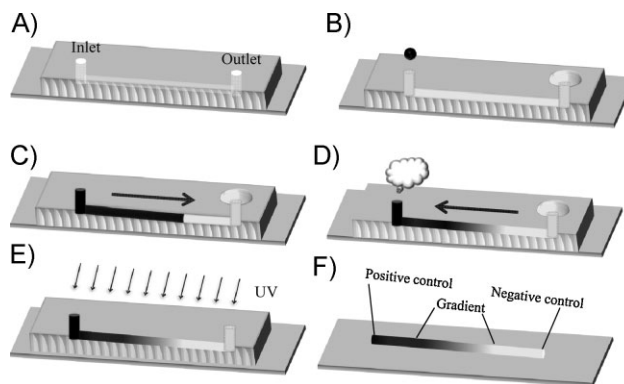


**Figure 1.** Schematic diagram of the gradient generation and stabilization by photopolymerization. A) The gradient generation device consists of a PDMS mold reversibly sealed to a TMS-PMA-treated glass slide. B) The channel was pre-filled with a low-concentration PEG-DA precursor from the outlet and a high-concentration PEG-DA precursor containing the chemicals of interest was introduced from the inlet. C) The solution of interest flowed spontaneously into the channel by a passive-pumping-induced forward flow. D) The gradient was generated by the combined effect of evaporation-induced backward flow and molecular diffusion. E) The gradient was stabilized by photopolymerization. F) The hydrogel gradient was obtained after demolding.

could be tuned by controlling the backward flow time. As shown in Figure 2A, when the solution was fully introduced into the channel, the flow profile was parabolic and the length of the gradient was about 4 mm. The parabolic profile gradually flattened in the first 5 min because of the evaporation-induced backward flow. As the backward flow continued, a centimeter-long

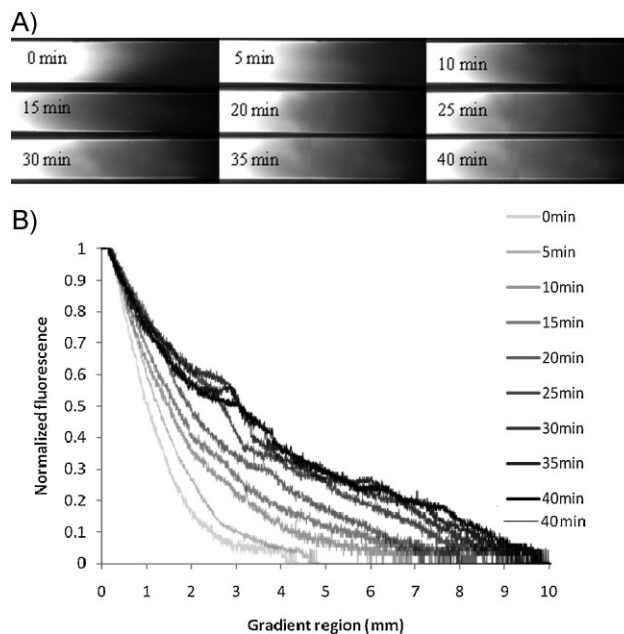


**Figure 2.** Investigation of the backward-flow time to regulate gradient formation. A) Fluorescent images to visualize the gradient at different backward-flow times. B) Normalized fluorescence distribution along the channel.

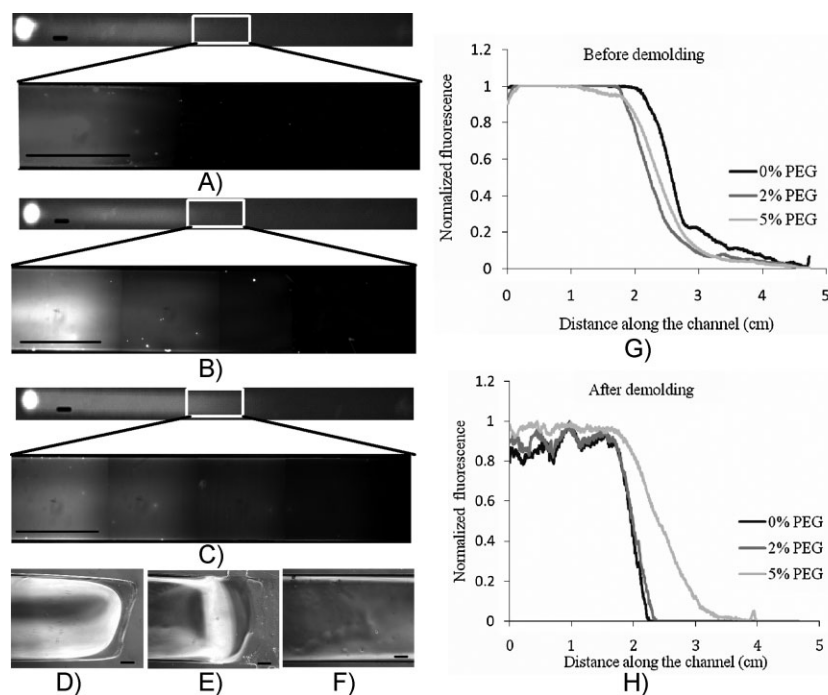


**Figure 3.** The effect of pre-filling precursor concentration on hydrogel-gradient formation (backward-flow time: 30 min). A–C) Fluorescent images of a hydrogel with 0%, 2% and 5% PEG-DA, respectively, as pre-filling solution after demolding; D–F) phase image of gradient hydrogels with 0%, 2% and 5% PEG-DA solution as pre-filling solution, respectively; G–H) normalized fluorescence distribution before and after demolding (scale bars in (a–c) 2 mm, scale bars in (d–f) 300  $\mu\text{m}$ ).

gradient could be generated within 30 min. Furthermore, the concentration formed an inverted parabolic profile. As shown in Figure 2B, when the backward flow time is longer than 30 min, there was little change in the gradient length. This was probably related to the low water-evaporation efficiency at an increasing solution concentration at the inlet. Therefore, a backward flow time of 30 min was selected for all subsequent experiments.

To form the hydrogel gradient, the hydrogel precursor solution was photopolymerized. The concentration of pre-filling solution was a key factor to ensure the integrity of the gradient in the final hydrogel after peeling off the PDMS mold. We pre-filled the channel with different concentrations of PEG-DA solution (0 wt %, 2 wt %, and 5 wt %), and then introduced 20 wt % PEG-DA containing 0.05 wt % rhodamine from the inlet to visualize the gradient formation. As shown in Figure 3A to C, for the 0 wt % and 2 wt % pre-filling solutions the rhodamine gradient disappeared immediately after demolding, but for the 5 wt % PEG-DA pre-filling solution, an intact hydrogel gradient could be obtained. Figure 3D to F show the phase images of the gradient regions generated for the three concentrations of pre-filling solution. As it can be seen, a hydrogel with a positive control region, a gradient region, and a negative control region could be generated only in the case of 5 wt %. The normalized-fluorescence distribution along the hydrogel, before and after demolding, was quantified using ImageJ software (Figure 3G and 3H). As it can be seen, the three

regions (positive control, gradient, and negative control) existed in all pre-filling solutions before demolding, and there was no significant difference in gradient profile. However, after demolding, a large portion of the gradient regions as well as the negative control regions were lost for the hydrogels with pre-filling PEG-DA concentrations of 0 wt % and 2 wt %.

To demonstrate the graded properties of the hydrogels generated from 5 wt % PEG-DA pre-filling solution and 40 wt % PEG-DA solution, the hydrogels were either air-dried or freeze-dried and subsequently visualized using scanning electron microscopy (SEM). During air-drying the water in the hydrogel gradually evaporated at room temperature and a film was created. During freeze-drying the hydrogel was frozen and then lyophilized to generate a porous material upon the sublimation of the ice crystals. Figure 4A shows representative SEM images of the three regions in the same air-dried hydrogel sample. A thinner layer was formed close to the outlet side with a graded intermediate layer in the middle and a thicker layer formed close to the inlet side. The thickness of the air-dried hydrogel sample at the 5 wt % PEG-DA side was about 5  $\mu\text{m}$  and that at the 40 wt % PEG-DA side was about 40  $\mu\text{m}$ . Figure 4B shows the porous structures of the freeze-dried hydrogel sample. As it can be seen, the porosity gradually increased from the inlet to the outlet. It should be noted that the viscosity of the hydrogel precursors may

influence the forward and backward flow and the resultant hydrogel gradient. Therefore, this may be a limitation of this technique as handling hydrogel precursors with high viscosity is difficult.

To demonstrate the bioactivity of the hydrogel gradient, we generated a gradient of hydrogel conjugated with adhesive RGDS ligands, and investigated the attachment of human umbilical vein endothelial cells (HUVECs). As shown in Figure 5A to C, the cell number and morphology were significantly different in the three regions of the hydrogel. At the positive control region containing 8.0 mm RGDS, many HUVECs attached and spread well on the hydrogel surface, whereas few cells attached to the negative control region because of the minimal protein adsorption on the hydrophilic PEG-DA surfaces. In the gradient region, the cell numbers follow a similar decreasing trend as the concentration of the RGDS ligands. A closer look at the cell morphology in the gradient region (Fig. 5D) shows that in the lower RGDS concentration region, the cells remained round in shape with little spreading, whereas towards the higher RGDS concentration region they tend to spread out more.

The cell number and spreading area along the hydrogel were quantified as shown in Figure 5E and 5F. The same trend was observed as before: at the positive control region a higher cell attachment can be seen, a gradually decreasing cell attachment is found at the gradient region, and a lower cell attachment is apparent at the negative control region. The cell density for the positive

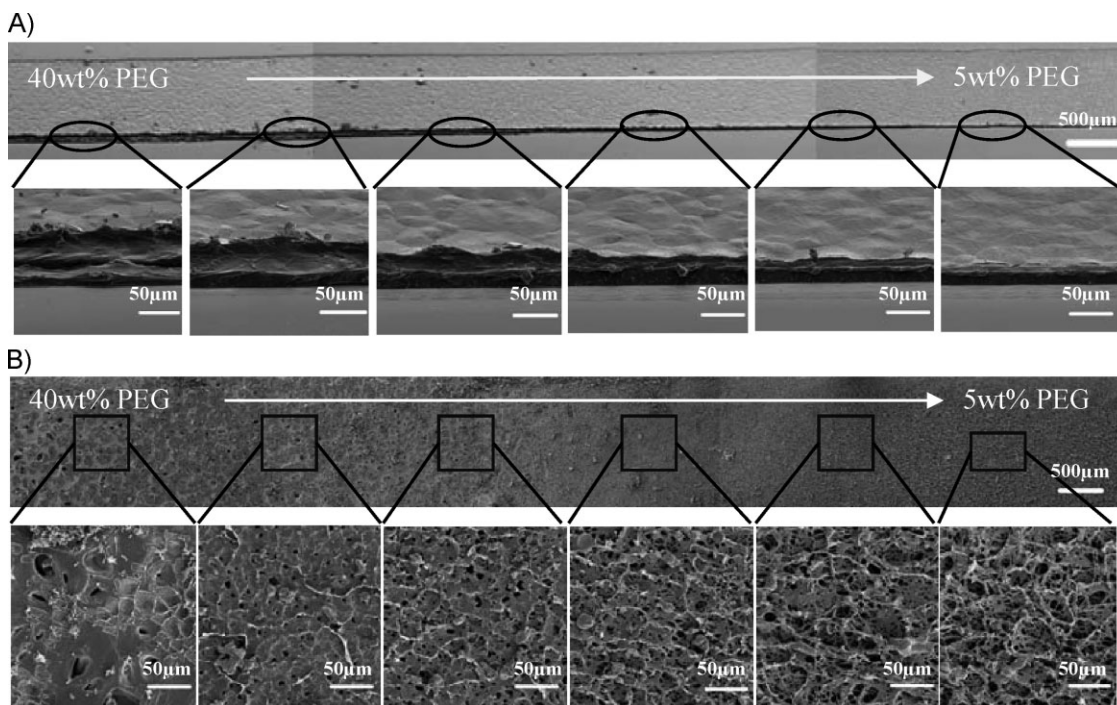


**Figure 4.** Characterization of air-dried and freeze-dried PEG-DA concentration-gradient hydrogels. A) SEM images of the cross sections of the air-dried hydrogels in the gradient region. B) SEM images of the freeze-dried hydrogel in the porosity-gradient region.

control region was  $93 \pm 7$  cells  $\text{mm}^{-2}$ , and the cell spreading area was  $842 \pm 136 \mu\text{m}^2$ , while at the negative control region, there were few cells and the cell spreading area was  $271 \pm 41 \mu\text{m}^2$ . For the gradient region, the larger error bars indicate that the HUVECs are distributed in a gradient manner, which is further validated by the quantification of the cell number in the gradient region (Fig. 5G). Moreover, the concentration of RGDS tethered to the hydrogel also affected the cell-spreading area as shown in Figure 5H.

To investigate the effect of the PEG-DA concentration gradient on cell behavior, we generated gradient hydrogels ranging from 30 wt % PEG-DA to 5 wt % PEG-DA with a uniform concentration (5.0 mm) of Acr-PEG-RGDS. As shown in Figure 6A, the cell morphology in the different regions of the hydrogel was significantly different. In the negative control region (5 wt % PEG-DA), the cells were round in shape and did not spread. In contrast, in the positive control region (30 wt % PEG-DA), the cells were well-spread and appeared to be well-adhered to the underlying substrate. Most notably, the morphology of the cells located in the gradient regions gradually changed from round to well-spread. We also quantified the cell-spreading area in the three regions of the hydrogel. The results (Fig. 6B) show that the average cell-spreading area in the gradient region was  $705 \pm 273 \mu\text{m}^2$  and those for the positive control and negative control regions were  $662 \pm 71 \mu\text{m}^2$  and  $316 \pm 19 \mu\text{m}^2$ , respectively. In the gradient region the cell-spreading area gradually increases in a gradient manner (Fig. 6C). However, it should be noted that the cell number attached to the hydrogel increased with a decrease in PEG-DA concentration, which was also observed for cells that were cultured on hydrogels with constant PEG-DA concentrations (5 wt %, 15 wt %, and 30 wt %) (see Supporting Information).

### 3. Discussion

The goal of the present study was to develop a simple, rapid, and versatile approach for the generation of stable long-range gradient hydrogels using a microfluidic method. Several features of the current approach for gradient generation distinguish it from existing methods: 1) the resultant hydrogel gradient has three different regions: a positive control, a negative control, and a gradient region; which provides a high-throughput platform for biological studies with little experimental error; 2) the size of the hydrogel gradient is on the centimeter length scale; 3) the generation of the gradient is rapid (within 30 min), highly dynamic (through the backward flow stage), and spatially/temporally controllable (by controlling the evaporation-induced backflow); 4) the gradient can be formed by using only low amounts of the molecules of interest (about 2 to 6  $\mu\text{L}$  for the current microfluidic channel design); and 5) the approach is simple and highly reproducible in a portable microfluidic device, requiring only a pipette for implementation.

We have shown that to maintain the integrity of the hydrogel gradient, the concentration of pre-filling PEG-DA solution should be at least 5 wt % for photopolymerization. On the other hand, to generate the gradient profile in the final hydrogel as predicted by using rhodamine, the concentration of PEG-DA solution should be less than 40 wt %. Higher concentrations of PEG-DA solution were too viscous to fill the microfluidic channel by our surface-tension driven process. However, it is possible to use higher concentrations by simple modifications to the experimental procedures, such as, by using a syringe pump. In this study, we have successfully created a gradient hydrogel with 40 wt % and 5 wt % PEG-DA concentrations. When the

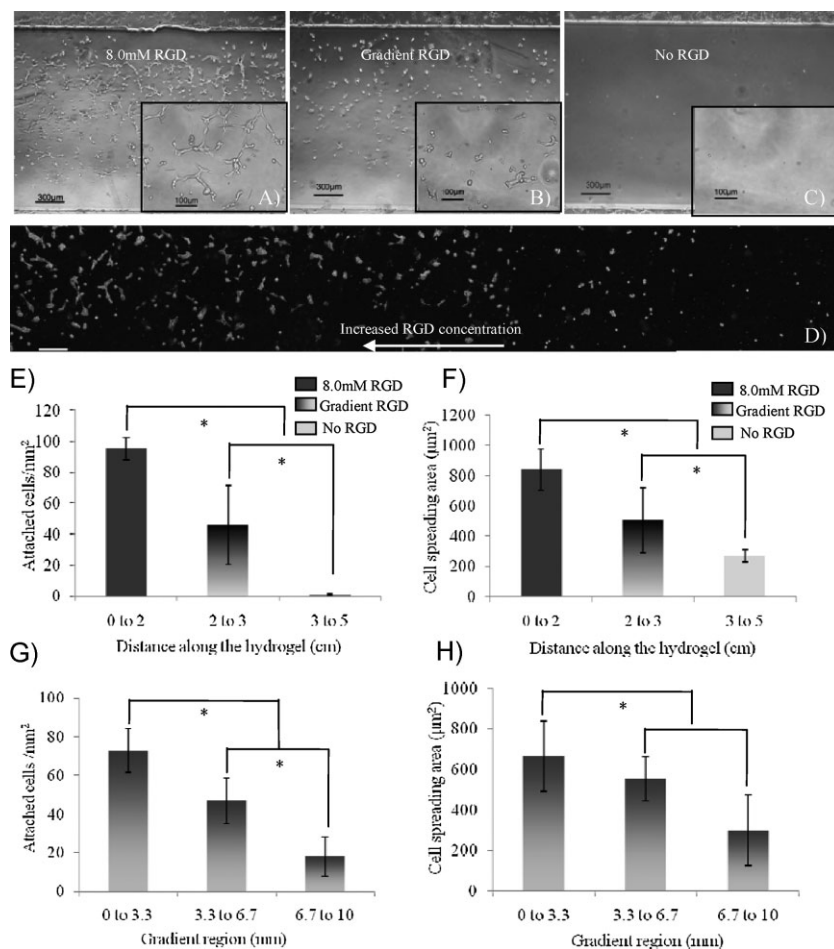


**Figure 5.** Generation of RGDS-gradient hydrogel to guide HUVECs attachment and spreading. A) Positive control regions with 8.0 mM RGDS. B) RGDS-gradient regions. C) Negative control regions without RGDS. D) Phase images of endothelial cells on RGDS-gradient hydrogel (scale bar: 200  $\mu\text{m}$ ). E,F) Quantification of cell number and spreading area along the hydrogel. G,H) Quantification of cell number and spreading area in gradient region ( $* = p < 0.05$ ).

hydrogel was freeze dried, a porous scaffold was generated with gradient porosity. This may be of particular importance for engineering tissues with gradient porous structures and material distributions, such as cartilage.<sup>[30]</sup> It can be envisioned that a functional scaffold with different biomaterial distribution and gradient porous structures could be fabricated by combining the presented gradient-generation method with a freeze-drying method. Moreover, it is possible to incorporate bioactive molecules or proteins (e.g., growth factors) into the porous scaffolds in a controlled manner.

Cellular behaviors, such as adhesion and spreading, are largely regulated by the presence of adhesive molecules. To address these issues, we first generated a RGDS gradient in the cell-repellent PEG-DA hydrogels. The HUVECs cultured on the chemical gradient hydrogel show dramatically different responses dependent on whether they are located on the positive control, the gradient, or the negative control region in the same hydrogel. Especially in the gradient region, the cell number gradually increased with the addition of RGDS peptide.

For the hydrogels with the gradient PEG-DA concentrations, we found that the morphology of the cells located on the gradient regions gradually changed from round to well-spread, which corresponds well with what has been reported previously for vascular smooth muscle cells cultured on hydrogels with a concentration gradient of polyacrylamide.<sup>[5]</sup> However, the cell number attached on the hydrogels showed an opposite trend in comparison to the cell-spreading area. The negative effect of PEG-DA concentration on cell attachment might be attributed to the blocking effect of PEG-DA on the RGDS ligand exposed to cells cultured on the hydrogel. Since PEG is well known for its blocking effect on bioactive surfaces, higher PEG-DA concentrations may lead to a relatively lower RGDS ligand-density exposure to cells on the hydrogel surface.

## 4. Conclusions

We have presented a simple and versatile approach to rapidly generate biologically relevant hydrogels with a chemical gradient by combining passive-pump induced forward flow, evaporation-induced backward flow, and photopolymerization techniques in a microfluidic channel. The parameters affecting the generation of a gradient hydrogel were investigated, such as, the backward flow time and the lowest concentration of pre-filling PEG-DA solution. The resultant hydrogel contains a positive control region, a gradient region, and a negative control region, which makes the experimental results more accurate and comparable. Porous tissue-engineering scaffolds with gradient porosity variation could be generated by freeze drying the hydrogel with the PEG-DA concentration gradient. The response of endothelial cells (adhesion and spreading) to the resultant chemical gradient hydrogels further validated that the presented gradient-hydrogel-generation method is a promising platform to study biological processes such as cell migration and cell-material interactions.

## 5. Experimental

**Materials:** PEG-DA ( $M_w$  4000) was purchased from Monomer-Polymer & Dajac Labs and Acr-PEG-RGDS was synthesized as described previously [31,32]. Briefly, Gly-Arg-Gly-Asp-Ser (GRGDS) ( $1 \text{ mg mL}^{-1}$ , Bachem) was reacted with an equimolar amount of acrylate-PEG-*N*-hydroxysuccinimide (3500 Da, Jenkem Technology) in a sodium bicarbonate buffer (50 mM, pH 8.2) for 2 h at room temperature. The product was dialyzed, freeze dried, and stored at  $-20^\circ\text{C}$  until use. The photoinitiator was 2-hydroxy-1-[4-(hydroxyethoxy)phenyl]-2-methyl-1-propanone (D2959, Ciba Geigy, at a concentration of 0.5 wt %). All other reagents were purchased from Sigma-Aldrich (St. Louis, MO) unless specifically mentioned.

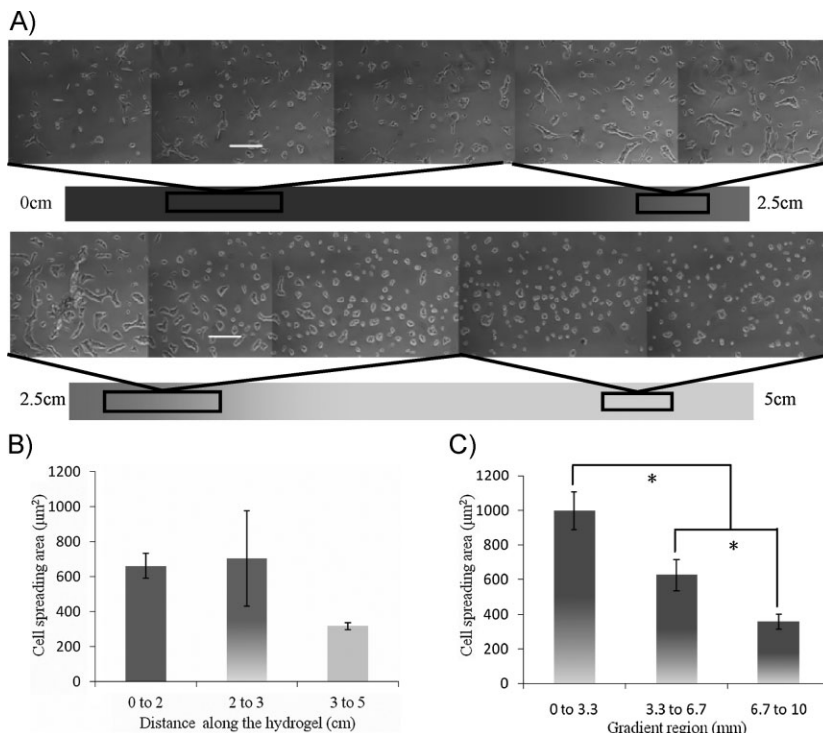


**Figure 6.** Hydrogels with PEG-DA concentration gradient and constant RGDs concentration to guide HUVECs spreading. A) Representative phase-contrast images to show the cell morphologies at different regions of a 5 cm-long hydrogel (scale bar: 200 µm). B) Quantification of the cell-spreading area along the PEG-DA concentration-gradient hydrogel. C) Quantification of the cell-spreading area in the gradient region ( $^* = p < 0.05$ ).

**Microfluidic Device:** The microfluidic device consisted of a PDMS mold with a straight fluidic channel (50 mm × 2.0 mm × 100 µm) and a bottom glass slide [29]. The PDMS mold was fabricated using standard soft-lithography methods and reversibly sealed to the glass coverslip. An inlet and outlet of the microchannel were created by a sharp punch (hole radius: 0.4 mm). The glass slide was pre-treated with 3-(trimethoxysilyl) propyl methacrylate (TMS-PMA) to create free methacrylate groups on the glass surface, which promoted the adhesion of PEG-DA hydrogels after UV exposure.

**Generation of Chemical Gradient Hydrogels:** The microchannel was initially introduced with the pre-filling solution, namely Dulbecco's Phosphate Buffered Saline (DPBS, Gibco, Carlsbad, CA) or a low-concentrated PEG-DA solution. Pre-filling solution (200 µL) was pipetted onto the outlet opening and PEG-DA solution (2 µL) with chemical molecules of interest or higher PEG-DA concentration was dropped onto the inlet opening. The difference of the surface tension between the two drops induced the automatic flow from inlet to outlet. Three drops of PEG-DA solution (2 µL) were introduced from the inlet. If the inlet was not refilled, the forward flow would stop and a backward flow would occur induced by the evaporation of the solution from the inlet at room humidity (30%). The pre-polymer concentration gradient was mainly developed during the backward-flow process. To visualize the dynamic process of the gradient formation, 0.05 wt % rhodamine was mixed with the PEG-DA solution in the inlet and a series of fluorescent images were captured every 5 min after backflow occurred using a fluorescent microscope (Nikon Eclipse TE2000-U, AVON, MA). The normalized fluorescence intensity in the gradient region was quantified using ImageJ software.

The specific hydrogel precursor with concentration gradient was stabilized in the final hydrogels upon photopolymerization (UV exposure: 10 mW cm<sup>-2</sup> for 70 s). To ensure the integrity of the gradient in the hydrogel, PEG-DA solutions with different concentrations (0 wt %, 2 wt %, and 5 wt %)

were used as the pre-filling solutions. The final gradient hydrogel was characterized by a Kodak Gel Logic 100 Imaging System (phase-contrast and fluorescent microscope). The normalized fluorescence-intensity distribution in the hydrogel before and after demolding was quantified using ImageJ software.

**Characterization of PEG-DA Concentration-Gradient Hydrogel:** To fabricate the PEG-DA concentration-gradient hydrogel, a PEG-DA solution (40 wt %) was used as the drop solution (2 µL) and another PEG-DA solution (5 wt %) was selected as pre-filling solution. The resultant hydrogels were air-dried, cut with a scalpel blade to obtain a cross section, sputter-coated with gold, and imaged using SEM (ULTRA 55, ZEISS). Freeze drying of the gradient hydrogel created a porous scaffold with porosity gradient.

**Fabrication of RGDs-gradient Hydrogel to Guide Cell Attachment:** To create an Acr-PEG-RGD gradient hydrogel for cell-attachment studies, a 20 wt % PEG-DA solution was first dropped into the microchannel and three drops of a PEG-DA solution (20 wt %, 2 µL) containing Acr-PEG-RGDs (8.0 mm) were introduced into the inlet. HUVECs were cultured in endothelial cell basal medium (EBM-2, Clonetics) supplemented with vascular endothelial growth factor (VEGF, 0.5 mL), hydrocortisone (0.2 mL), epidermal growth factor (rhEGF, 0.5 mL), ascorbic acid (0.5 mL), r-human fibroblast growth factor-B (rhFGF-B, 2.0 mL), heparin (0.5 mL), recombinant long R insulin-like growth factor (R<sup>3</sup>-IGF-, 0.5 mL) and gentamicin sulfate amphotericin-B (GA-10000, 5 mL) at 37 °C in a humidified incubator. Upon trypsinization, the cells were seeded on the surface of the hydrogels with Acr-PEG-RGDs gradient, which were pre-washed five times in DPBS and twice in EBM-2. The cell seeding density was 4 × 10<sup>4</sup> cells cm<sup>-2</sup>. After 6 h of incubation, the hydrogels were rinsed three times with sterile PBS to wash away unattached cells and then visualized using a phase-contrast microscope. Cells were quantified by counting the attached-cell number in a minimum of eight images from three individual hydrogels.

**Cell Study on PEG-DA Concentration-Gradient Hydrogel:** To create the PEG-DA concentration-gradient hydrogel for cell study, a PEG-DA solution (5 wt %) was first dropped into the microchannel and three drops of another PEG-DA solution (30 wt %, 2 µL) were introduced into the inlet. To promote the adhesion of HUVECs onto the PEG-DA concentration-gradient hydrogel, Acr-PEG-RGDs (5.0 mm) was incorporated into both solutions. HUVECs were seeded onto the hydrogels at a density of 1 × 10<sup>4</sup> cells cm<sup>-2</sup>. After 24 h of incubation, the cells were fixed for 15 min in a glutaraldehyde solution (0.75% in PBS), and then observed under a phase-contrast microscope. The effect of PEG-DA concentration on the cell morphology was investigated.

**Statistical Analysis:** All quantitative data is expressed as mean ± standard deviation. Statistical analysis was performed using a one-way analysis of variance (ANOVA) and Tukey HSD tests for post-hoc comparison using the SPSS 14.0 statistical package (SPSS Inc. Chicago, USA). Values of  $p < 0.05$  were considered statistically significant.

## Acknowledgements

This research was funded by the US Army Engineer Research and Development Center, the Institute for Soldier Nanotechnology, and the NIH (HL092836 and DE019024). J. H. was partially sponsored by the China Scholarship Council (CSC), the Program for Changjiang Scholars and Innovative Research Team in University (IRT0646), China. We thank Lifeng Kang, Yi Dong, Adam Hacking, Behnam Zamanian, and Shahriar Hojjati Emami for the scientific and technical support. J. H. and Y. D. contributed equally to this work. J. H., Y. D., J. L. V., and A. K. designed the research

strategy; J. H., Y. D., and J. L.V. performed the experiments; J. H., Y. D., and C. H. analyzed the data; J. H., Y. D., D. L., and A. K. wrote the paper. Supporting Information is available online from Wiley InterScience or from the authors.

Received: July 16, 2009

Published online: November 24, 2009

- [1] A. Khademhosseini, R. Langer, J. Borenstein, J. P. Vacanti, *Proc. Natl. Acad. Sci. USA* **2006**, *103*, 2480.
- [2] J. A. Burdick, A. Khademhosseini, R. Langer, *Langmuir* **2004**, *20*, 5153.
- [3] A. J. Engler, S. Sen, H. L. Sweeney, D. E. Discher, *Cell* **2006**, *126*, 677.
- [4] M. P. Lutolf, J. A. Hubbell, *Nat. Biotechnol.* **2005**, *23*, 47.
- [5] N. Zaarl, P. Rajagopalan, S. K. Kim, A. J. Engler, J. Y. Wong, *Adv. Mater.* **2004**, *16*, 2133.
- [6] N. A. Peppas, J. Z. Hilt, A. Khademhosseini, R. Langer, *Adv. Mater.* **2006**, *18*, 1345.
- [7] W. F. Liu, C. S. Chen, *Mater. Today* **2005**, *8*, 28.
- [8] N. J. Sniadecki, A. Anguelouch, M. T. Yang, C. M. Lamb, Z. Liu, S. B. Kirschner, Y. Liu, D. H. Reich, C. S. Chen, *Proc. Natl. Acad. Sci. USA* **2007**, *104*, 14 553.
- [9] A. Harris, *Exper. Cell Res.* **1973**, *77*, 285.
- [10] B. K. Brandley, R. L. Schnaar, *Developm. Biol.* **1989**, *135*, 74.
- [11] C. M. Lo, H. B. Wang, M. Dembo, Y. Wang, *Biophys. J.* **2000**, *79*, 144.
- [12] J. Y. Wong, A. Velasco, P. Rajagopalan, Q. Pham, *Langmuir* **2003**, *19*, 1908.
- [13] M. Wang, *Biomaterials* **2003**, *24*, 2133.
- [14] R. S. Langer, J. P. Vacanti, *Sci. Am.* **1999**, *280*, 86.
- [15] S. A. DeLong, A. S. Gobin, J. L. West, *J. Control. Release* **2005**, *109*, 139.
- [16] S. A. DeLong, J. J. Moon, J. L. West, *Biomaterials* **2005**, *26*, 3227.
- [17] C. T. Lo, D. J. Throckmorton, A. K. Singh, A. E. Herr, *Lab on a Chip* **2008**, *8*, 1273.
- [18] C. L. Hypolite, T. L. McLernon, D. N. Adams, K. E. Chapman, C. B. Herbert, C. C. Huang, M. D. Distefano, W. S. Hu, *Bioconjugate Chem.* **1997**, *8*, 658.
- [19] C. B. Herbert, T. L. McLernon, C. L. Hypolite, D. N. Adams, L. Pikus, C. C. Huang, G. B. Fields, P. C. Letourneau, M. D. Distefano, W. S. Hu, *Chem. Biol.* **1997**, *4*, 731.
- [20] S. T. Plummer, P. W. Bohn, *Langmuir* **2002**, *18*, 4142.
- [21] E. L. Ratcliff, A. C. Hillier, *Langmuir* **2007**, *23*, 9905.
- [22] J. D. Whittle, D. Barton, M. R. Alexander, R. D. Short, *Chem. Commun.* **2003**, 1766.
- [23] M. R. Alexander, J. D. Whittle, D. Barton, R. D. Short, *J. Mater. Chem.* **2004**, *14*, 408.
- [24] B. Chu, D. Liang, *Electrophoresis* **2002**, *23*, 2602.
- [25] D. Liang, L. Song, M. A. Quesada, Z. Tian, F. W. Studier, B. Chu, *Electrophoresis* **2000**, *21*, 3600.
- [26] N. L. Jeon, S. K. W. Dertinger, D. T. Chiu, I. S. Choi, A. D. Stroock, G. M. Whitesides, *Langmuir* **2000**, *16*, 8311.
- [27] S. K. Dertinger, X. Jiang, Z. Li, V. N. Murthy, G. M. Whitesides, *Proc. Natl. Acad. Sci. USA* **2002**, *99*, 12 542.
- [28] S. Weiner, H. D. Wagner, *Annu. Rev. Mater. Sci.* **1998**, *28*, 28.
- [29] Y. Du, J. Shim, M. Vidula, M. J. Hancock, E. Lo, B. G. Chung, T. Borenstein, M. Khabiry, D. M. Cropek, A. Khademhosseini, *Lab Chip* **2009**, *9*, 761.
- [30] T. B. Woodfield, C. A. Van Blitterswijk, J. De Wijn, T. J. Sims, A. P. Hollander, J. Riesle, *Tissue Eng.* **2005**, *11*, 1297.
- [31] J. A. Burdick, K. S. Anseth, *Biomaterials* **2002**, *23*, 4315.
- [32] D. L. Hern, J. A. Hubbell, *J. Biomed. Mater. Res.* **1998**, *39*, 266.